Experimental characterization of true spontaneous emission rate of optically-pumped InGaAs/GaAs quantum-well laser structure

Q.-N. Yu, Y. Jia, W. Lu, M.-Q. Wang, F. Li, J. Zhang, X. Zhang, Y.-Q. Ning, and J. Wu

---

Articles you may be interested in

Experimental characterization of true spontaneous emission rate of optically-pumped InGaAs/GaAs quantum-well laser structure

Q.-N. Yu,[1] Y. Jia,[1] W. Lu,[1] M.-Q. Wang,[1] F. Li,[1] J. Zhang,[2] X. Zhang,[2] Y.-Q. Ning,[2] and J. Wu[1,a]

[1]*Department of Applied Physics, Beihang University, Beijing 100191, China*
[2]*State Key Laboratory of Luminescence and Application, Changchun Institute of Optics, Fine Mechanics and Physics, Chinese Academy of Sciences, 130033 Changchun, China*

In this paper, an experimental approach to acquiring true spontaneous emission rate of optically-pumped InGaAs/GaAs quantum-well laser structure is described. This method is based on a single edge-emitting laser chip with simple sample processing. The photoluminescence spectra are measured at both facets of the edge-emitting device and transformed to the spontaneous emission rate following the theory described here. The unusual double peaks appearing in the spontaneous emission rate spectra are observed for the InGaAs/GaAs quantum-well structure. The result is analyzed in terms of Indium-rich island and Model-Solid theories. The proposed method is suitable for electrically-pumped quantum-well laser structures, as well. © *2017 Author(s).* *All article content, except where otherwise noted, is licensed under a Creative Commons Attribution (CC BY) license (http://creativecommons.org/licenses/by/4.0/).* [http://dx.doi.org/10.1063/1.4990630]

Optically-pumped InGaAs/GaAs quantum well structure has been demonstrated to be of great potentials for many laser applications, e.g. tunable semiconductor lasers,[1] optical pumping sources[2] and vertical-external-cavity surface-emitting lasers, etc.[3–7] In design and investigation of InGaAs/GaAs quantum well lasers, an important physical parameter, i.e. the spontaneous emission rate (SER) is necessary to be known because it characterizes laser material lightening mechanism. The parameter of SER is generally obtained by theoretical calculation at present.[8–10] Since the theoretical result fails to contain the influence from structure defects in the device, it cannot exactly present the true SER spectrum and reflects only ideal performance of the device. This can be clearly seen in the subsequent results in this paper. Therefore, it is significant to acquire the true SER spectra of semiconductor lasers by experimental measurement. Unfortunately, most previous experimental investigations on the spontaneous emission focused only on the spontaneous emission intensity, rather than spontaneous emission rate,[11–16] especially on the spontaneous emission rate spectrum.

In this paper, an experimental approach to acquiring the true SER spectrum of the optically-pumped InGaAs/GaAs quantum-well laser structure is proposed. The method is simple and effective, as it does not need complicated sample processing. The true SER spectra with dual peaks due to special InGaAs/GaAs quantum-well structure are observed and analyzed. The method is described below.

In order to obtain SER spectrum of the InGaAs/GaAs quantum well laser structure, the photoluminescence (PL) spectra are measured at both facets of a single edge-emitting laser chip. The principle to obtain PL spectra is illustrated in Fig. 1.

The reflectivity of the two facets are designed to be $R_1=0$ and $R_2=R$, respectively. L and P denote lens and polarizer, respectively. 808nm laser is used as the pump source. I_{PL1} and I_{PL2} are the PL spectral intensities measured at both facets of the device. The relation between the spontaneous

---

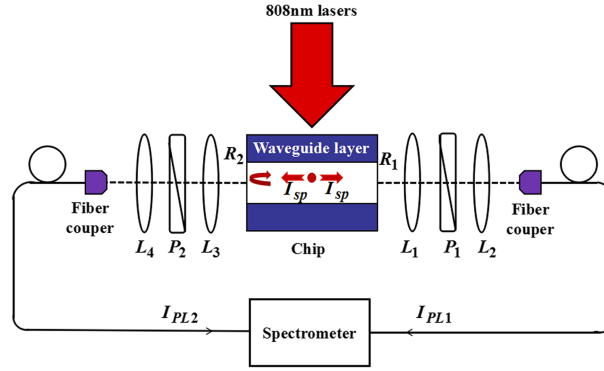[a]Electronic mail: jwu2@buaa.edu.cn.

7, 085319-1

FIG. 1. Schematic diagram of SER measurement based on PL spectra from dual facets of the laser device.

emission intensity, I_{sp} and PL spectral intensities can be established as[17]

$$I_{PL1} = \frac{I_{sp}}{G}\left(e^{GL} - 1\right)\left(\mathrm{Re}^{GL} + 1\right) \tag{1}$$

$$I_{PL2} = \frac{(1-R)I_{sp}}{G}\left(e^{GL} - 1\right) \tag{2}$$

where L is the laser medium length and G denotes modal gain of the well. The spontaneous emission intensity, I_{sp} can be expressed by removing modal gain in the equations (1) and (2).

$$I_{sp} = \frac{RI_{PL2}^2}{L\left[(1-R)^2 I_{PL1} - (1-R^2)\,I_{PL2}\right]}\ln\frac{(1-R)\,I_{PL1} - I_{PL2}}{R \times I_{PL2}} \tag{3}$$

In theory, SER can be expressed as[18]

$$r_{sp}\left(hv\right) = \frac{m_r u\left(hv - E_g\right)}{\tau_r \pi \hbar^2 d}\exp\left(\frac{E_{fn} - E_{fp} - hv}{k_B T}\right) \tag{4}$$

where m_r denotes the reduced mass of an electron-hole pair and d is the quantum-well thickness. E_g is the effective band gap and τ_r denotes the radiative recombination lifetime. $u(hv - E_g)$ is the step function. E_{fn} and E_{fp} represent the Fermi levels of conduction band and valence band, respectively. T is the temperature and hv denotes photon energy. k_B is the Boltzmann constant and *h* is the Planck's constant. In order to obtain the SER spectrum from experiment, an inversion factor P_F is introduced to the equation (4). It is written as[19]

$$P_F = \left[1 - \exp\left(\frac{hv - \Delta E_f}{kT}\right)\right] \tag{5}$$

where $\Delta E_f = E_{fn} - E_{fp}$ denotes the Fermi level separation between conduction band and valence band. Substituting the equation (5) into the equation (4) yields

$$r_{sp}\left(hv\right) = \frac{m_r u\left(hv - E_g\right)}{\tau_r \pi \hbar^2 d}\left(\frac{1}{1 - P_F}\right) \tag{6}$$

where the inversion factor P_F can also be expressed as

$$P_F = \frac{1}{C}\frac{1}{\Gamma}\left(\frac{2n^2 h^2 v^2}{3\pi^2 \hbar^3 c^2}\right)\left[\frac{G}{I_{sp}}\right] = A\frac{G}{I_{sp}} \tag{7}$$

where C is the scaling factor and Γ is the optical confinement factor relating to the quantum well structure, c is the speed of light in vacuum and n is the refractive index of the well materials. All the constants in the equation (7) are available and involved in the coefficient A here. By assuming that the carrier distributions are fully inverted at low photon energies, the scaling factor C

can be obtained. Combining the equations (1), (2), (3) and (7), the inversion factor, P_F can be described as

$$P_F = A \frac{(1-R)^2 I_{PL1} - \left(1-R^2\right) I_{PL2}}{R \times I_{PL2}^2} \tag{8}$$

By substituting the equation (8) into the equation (6), SER is obtained as

$$r_{sp}(h\nu) = \frac{BRI_{PL2}}{RI_{PL2}^2 - A(1-R)^2 I_{PL1} + A(1-R)^2 I_{PL2}} \tag{9}$$

where $B = m_r u(h\nu - E_g)/\tau_r \pi \hbar^2 d$ is the constant and available. Thus, SER can be obtained, as long as the PL spectra of I_{PL1} and I_{PL2} are known.

The wafer of experimental devices is grown by Metal organic Chemical Vapor Deposition (MOCVD). The edge-emitting sample size is 0.5mm × 1.5mm in area. The designed active layer of the device is a compressively-strained $In_{0.17}Ga_{0.83}As$ quantum well with a thickness of 10-nm, which is sandwiched by 8nm-thick $GaAs_{0.92}P_{0.08}$ barriers. A 2nm-thick GaAs strain-compensating layer is embedded between the well and the barrier. The waveguide layer is AlGaAs with a thickness of 2μm. One facet of the edge-emitting device is coated with the transmittance of T = 99.99%. The other facet of the device is uncoated, the reflectivity, R of which is determined by the material index. The well is vertically pumped from fiber-coupled 808nm pulsed laser under room temperature. The pump beam is reshaped from Gaussian pattern to flat-top one to generate fixed carrier density and gain distribution in the axial direction. With a linear polarizer, the PL spectra in transverse electric (TE) and transverse magnetic (TM) polarizations are measured. The results are shown in Fig. 2.

Thus, with the equation (9), the SER spectra in both TE (solid lines) and TM (dash lines) polarizations can be obtained, which are shown in Fig. 3. The dual peaks are observed in both TE and TM SER spectra and they are marked using letters A, B and C, D for TE and TM SERs, respectively. The maximum of SERs as functions of carrier densities for TE and TM modes are plotted in Fig. 4, respectively. The difference between TE and TM SERs indicates that the InGaAs/GaAs quantum-well structure is compressively strained, as the TM polarization-generated photon energy corresponding to the point, D is larger than the TE polarization -generated one corresponding to the point, A.

The dual peak phenomenon in Figs. 2 and 3 should be associated with Indium-rich island effect happening in the process of $In_xGa_{1-x}As$/GaAs material growth.[20] The $In_xGa_{1-x}As$ /GaAs structure is a sort of highly-strained material system due to a larger lattice mismatching value. Hence, some small clusters of Indium atoms are generated on the surface of $In_xGa_{1-x}As$ layer to relax high stress in the
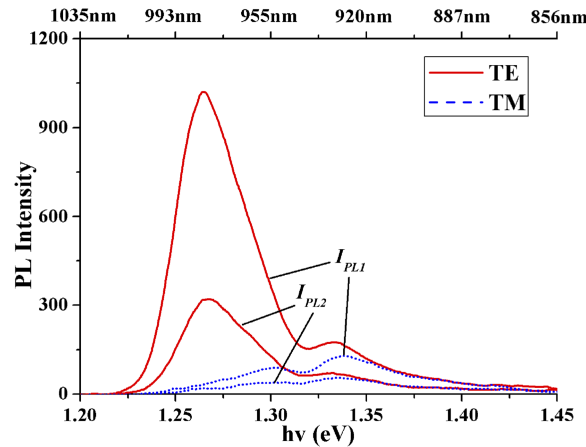

FIG. 2. PL spectra in TE and TM polarizations from both facets of the optically-pumped edge-emitting $In_{0.17}Ga_{0.8}3As$ quantum well device.
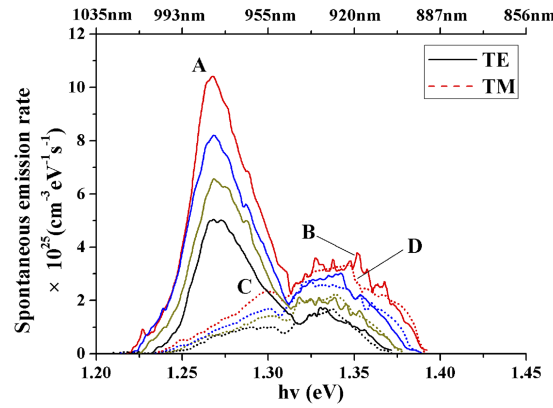
FIG. 3. SER spectra in TE and TM polarizations with various carrier densities of 3.6×10^{17} cm^{-3}, 4.2×10^{17} cm^{-3}, 4.5×10^{17} cm^{-3} and 4.8×10^{17} cm^{-3} from In$_{0.17}$Ga$_{0.83}$As/GaAs well structure.
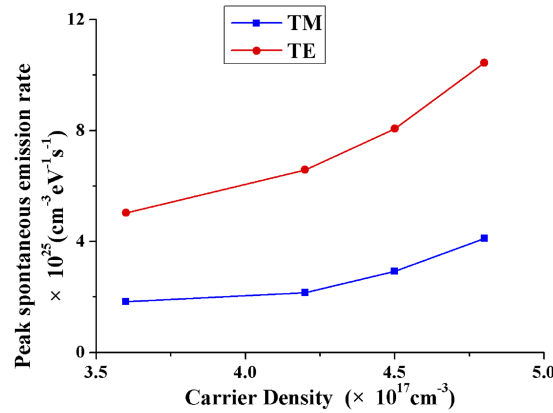

FIG. 4. The maximum of SERs as functions of carrier densities for TE and TM polarizations.

process of the material growth. As a result, the Indium atoms are migrating to the clusters because these clusters are of lower potential energy. Since the migration length of Indium atoms is much larger than that of Gallium atoms,[21] the smaller clusters of Indium atoms gradually accumulate and finally form Indium-rich islands on the surface of In$_x$Ga$_{1-x}$As layer. The migration of Indium atoms up to the surface of In$_x$Ga$_{1-x}$As layer and the formation of Indium-rich islands result in the reduction of Indium content in the subsurface of the In$_x$Ga$_{1-x}$As material system so that some Indium-reduced regions around the islands emerge for the In$_x$Ga$_{1-x}$As quantum well layer. This can be understood as a sort of surface defect for the quantum well from the material growth. Obviously, it is difficult to obtain the actual SER spectra reflecting the influence from structure defects, such as Indium-rich islands, with a pure theoretical approach.

In terms of Model-Solid theory,[22] the dual peaks in SER spectra in Fig. 3 are just corresponding to the Indium contents of x=0.17 and x=0.12 for the In$_x$Ga$_{1-x}$As/GaAs material system, respectively. This means that a sort of hybrid In$_x$Ga$_{1-x}$As well structure that contains both In$_{0.17}$Ga$_{0.83}$As and In$_{0.12}$Ga$_{0.88}$As is formed due to the Indium-rich island effect. A diagram to illustrate such a band structure and wave functions in both the first conduction sub-band (C$_1$) and the first valence sub-band for heavy holes (HH$_1$) and light holes (LH$_1$) is plotted with different Indium contents of In$_x$Ga$_{1-x}$As materials. It is shown in Fig. 5. The lattice mismatching between In$_x$Ga$_{1-x}$As/GaAs/GaAsP materials lead to a special hybrid strain structure, i.e. the compressive strain occurs in In$_{0.17}$Ga$_{0.83}$As and the bottom GaAs layers, as well as the tensile strain occurs in In$_{0.12}$Ga$_{0.88}$As and the inner GaAs layers. This results in specially-slanted band edges, as shown in Fig. 5. This special band structure makes carriers easier to move into the well and increases the carrier recombination rate.
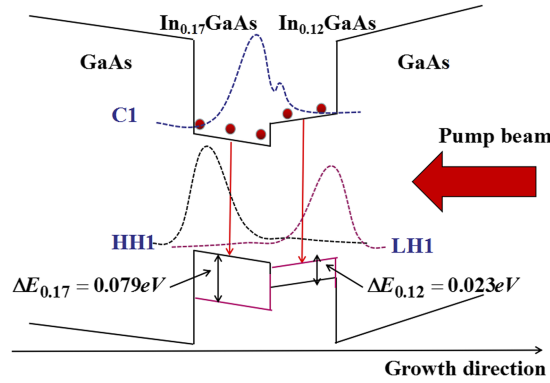
FIG. 5. Hybrid band structure and wave functions in the first conduction sub-band (C_1) and the first valence sub-band of heavy holes (HH_1) and light holes (LH_1) due to different Indium contents in $In_xGa_{1-x}As$ well.

Theoretically, the SER in TE polarization is mainly determined by the electron-hole recombination between the conduction band and the HH_1 band, while the SER in TM polarization is mainly associated with the electron-hole recombination between the conduction band and the LH_1 band.[23] Thus, the space between the maximum of TE and TM SERs is corresponding to the difference between the first sub-bands of HH_1 and LH_1. For $In_{0.17}Ga_{0.83}As$ materials, the band offsets for HH_1 and LH_1 are $\Delta E_{hh} = 0.025eV$ and $\Delta E_{lh} = -0.0544eV$. Thus, the difference between the first sub-band of HH_1 and LH_1 is $\Delta E_{0.17} = 0.079eV$. For $In_{0.12}Ga_{0.88}As$ materials, the band offsets for HH_1 and LH_1 are $\Delta E_{hh} = -0.0073eV$ and $\Delta E_{lh} = 0.0161eV$, respectively. So the separation between the first sub-band of HH_1 and LH_1 is $\Delta E_{0.12} = 0.023eV$.

The data and analysis presented above illustrate that the main peaks marked by A and D in both TE and TM SER curves in Fig. 3 occur due to the compressively-strained $In_{0.17}Ga_{0.83}As$/GaAs layer. The corresponding TE photon energy is less than TM photon energy. Meanwhile, the sub-peaks marked by B and C in both TE and TM SER curves in Fig. 3 occur due to the tensile strained $In_{0.12}Ga_{0.88}As$/GaAs region. The corresponding TE photon energy is larger than TM photon energy. From the results in Fig. 3, it can be seen that the SER values from $In_{0.17}Ga_{0.83}As$/GaAs layers are larger than those from $In_{0.12}Ga_{0.88}As$/GaAs region under the same carrier density for both TE and TM modes. This is because the carriers initially occupy energy levels in the $In_{0.17}Ga_{0.83}As$ layer due to the lower C_1 potential so that the carrier recombination happens prior in there, as illustrated in Fig. 5.

In summary, an experimental approach to acquiring both TE and TM spontaneous emission rates of optically-pumped $In_xGa_{1-x}As$/GaAs quantum-well laser structure is proposed in this paper. The method is based on the PL spectrum measurement at both facets of an edge-emitting laser device. The special dual peak configuration in the SER spectra from the $In_xGa_{1-x}As$/GaAs quantum-well structure is observed. Our analysis reveals that a special well structure containing some randomly-distributed $In_{0.12}Ga_{0.88}As$ regions on the surface of $In_{0.17}Ga_{0.83}As$ layer is formed. This is probably caused due to the Indium-rich island effect generated in the process of the material growth. This special well structure shows a hybrid strain feature, i.e. the compressive and tensile strains exist simultaneously for the well. The results will be very helpful to investigating and analyzing defects and performance of semiconductor lasers.

[1] L. Fan, M. Fallahi, J. T. Murray, R. Bedford, Y. Kaneda, J. Hader, A. R. Zakharian, J. V. Moloney, S. W. Koch, and W. Stolz, Appl. Phys. Lett. **88**, 021105 (2006).
[2] Q. W. Wang, J. Li, J. Y. Lin, and H. X. Jiang, Appl. Phys. Lett. **109**, 152103 (2016).
[3] M. Kuznetsov, F. Hakimi, R. Sprague, and A. Mooradian, IEEE J. Sel. Top. Quantum Electron. **5**, 561 (1999).
[4] S. Lutgen, T. Albrecht, P. Brick, W. Reill, J. Luft, and W. Spath, Appl. Phys. Lett. **82**, 3620 (2003).
[5] J. Chilla, S. Butterworth, A. Zeitschel, J. Charles, A. Caprara, M. Reed, and L. Spinelli, Proc. SPIE **5332**, 151 (2004).
[6] A. C. Tropper, H. D. Foreman, A. Garnache, K. G. Wilcox, and S. H. Hoogland, J. Phys. D **37**, R75 (2004).

[7] L. Fan, M. Fallahi, J. Hader, A. R. Zakharian, M. Kolesik, J. V. Moloney, T. Qiu, A. Schulzgen, N. Peyghambarian, S. W. Koch, W. Stolz, and J. T. Murray, Appl. Phys. Lett. **86**, 211116 (2005).

[8] L. Wang, R. Li, Z. Yang, D. Li, T. Yu, N. Liu, L. Liu, W. Chen, and X. Hu, Appl. Phys. Lett. **95**, 211104 (2009).

[9] S. H. Park, Y. T. Moon, J. S. Lee, H. K. Kwon, and J. S. Park, Phys. Stat. Sol. A. **208**, 195 (2011).

[10] J. Zhang and N. Tansu, J. Appl. Phys. **110**, 113110 (2011).

[11] A. Schönfelder, J. D. Ralston, K. Czotscher, S. Weisser, J. Rosenzweig, and E. C. Larkins, J. Appl. Phys. **80**, 582 (1996).

[12] I. Lyubomirsky, Q. Hu, and M. R. Melloch, Appl. Phys. Lett. **73**, 3043 (1998).

[13] S. E. Brinkley, Y.-D. Lin, A. Chakraborty, N. Pfaff, D. Cohen, J. S. Speck, and S. Nakamura, Appl. Phys. Lett. **98**, 011110 (2011).

[14] R. F. M. Hendriks, M. B. Willemsen, M. P. V. Exter, J. P. Woerdman, L. Weegels, K. H. Gulden, and M. Moser, Opt. Commun. **149**, 50 (1998).

[15] M. A. Duguay and T. C. Damen, Appl. Phys. Lett. **40**, 667 (1982).

[16] P. M. Smowton, P. Blood, and W. W. Chow, Appl. Phys. Lett. **76**, 1522 (2000).

[17] M.-L. Ma, J. Wu, Y.-Q. Ning, F. Zhou, M. Yang, X. Zhang, J. Zhang, and G.-Y. Shang, Opt. Express **21**, 10335 (2013).

[18] N. C. Chen, C. M. Lin, C. Shen, W. C. Lien, and T. Y. Lin, Opt. Express **16**, 20759 (2008).

[19] G. M. Lewis, P. M. Smowton, J. D. Thomson, H. D. Summers, and P. Blood, Appl. Phys. Lett. **80**, 1 (2002).

[20] D. Schlenker, T. Miyamoto, Z. Chen, F. Koyama, and K. Iga, J. Cryst. Growth. **209**, 27 (2000).

[21] R. Kaspi and K. R. Evans, Appl. Phys. Lett. **67**, 819 (2016).

[22] C. G. Van de Walle, Phys. Rev. B **39**, 1871 (1989).

[23] L. A. Coldren, *Diode Lasers and Photonic Integrated Circuits*, 2th ed (Wiley, Hoboken, 2012) p. 167.